Analysis of coatings which inhibit epoxy bleeding in electronic packaging

N. X. TAN, K. H. H. LIM, A. J. BOURDILLON*
*Hewlett Packard (ICBD), 2 Corporation Road, Singapore 2261 and *Department of Materials Science, National University of Singapore, Lower Kent Ridge Road, Singapore 0511*

The bleeding of epoxy resin around surfaces, undergoing bonding in electronic packaging assembly, has for long caused sporadic yield-loss. This loss is more severe in advanced and dense packages. Previously it has been supposed that the loss results from surface contaminants which are reduced by vacuum bakeout. In fact, that procedure generates coatings of hydrocarbons as we show by surface analysis. The coatings very strongly affect the wettabilities and measured surface energies of substrates. In particular, the comparatively low surface energy of hydrocarbon films on gold surfaces shows how the surfaces can be engineered, with coatings of ''appropriate cleanliness'', to systematically inhibit epoxy bleeding.

1. Introduction

Epoxy bleeding is commonly observed in electronic packages around silicon chips attached with epoxy resin to substrates having gold or other metal surfaces. In severe cases the bleeding causes failure due to contamination at wire bond pads. The effects of bleeding are often critical in advanced packaging components such as ceramic pin grid array (CPGA) substrates. In particular, when there exists a close clearance between a bond finger tier and the die, minor resin bleedout can interfere with wire bondability. Earlier studies [1] have led to countermeasures, chiefly by vacuum baking. However, the analysis was incomplete and yield-losses continue to occur from time to time for no apparent reason. In addition up to now it appears that no one has addressed the possibility of surface contamination, caused by vacuum baking, having a positive effect such as lower epoxy bleeding during die attachment. Here we provide a more complete analysis by investigating the effects of vacuum baking through surface analysis and contact angle measurements.

The die attach pad on the CPGA [2] substrate consisted of a Cu–W heat slug onto which was electroplated firstly a film of nickel, 10 μm thick, followed by gold, typically 1.2 μm thick. The surface was subsequently cleaned by standard procedures using isopropyl alcohol (IPA) and IPA vapour drying. When the thickness of the surface gold film was varied from 1 to 2 μm on different specimens, the wettability appeared to be independent of the gold thickness.

2. Experimental details

2.1. Auger analysis

Auger analysis was performed on a Jeol JAMP-7100E. The accelerating voltage was 5 kV. The probe current was about 1.52×10^{-7} A. Argon ion etching was applied with an etching speed estimated at 1.25 nm per 10 s on a silicon surface.

The analysis was carried out on substrates prepared for die attachment. Fig. 1 shows a schematic diagram of the substrates after die attachment but before wire bonding. Auger spectra were recorded from the die attach pads, or heat slugs, which consisted of copper electroplated with nickel and gold. Comparisons were made between samples at two stages along the process: before and after baking in vacuum or in air. The first purpose was to monitor any contamination during baking. Three samples from lot A consisted of (i) a raw CPGA substrate, (ii) a CPGA substrate after baking at 235 °C for 6 h in a conventional vacuum oven at a pressure of 0.1 mbar (10 Pa) and (iii) a CPGA substrate after baking in an air convection oven at 235 °C for 6 h. Measurements were taken from several specimens of each type and found to be consistent.

In order to investigate the formation of surface carbon contamination by either oil backstreaming in the vacuum or by diffusion of residues from subsurface pores, another group of CPGA substrates was investigated by placing a substrate in an oven which was evacuated but not thermally cycled. Samples were taken from lot B, nominally processed in the same way as lot A. The comparison allowed initial monitoring of expected variations from lot to lot, but only minor differences in contamination levels were observed. Two samples consisted of (i) a raw CPGA substrate and (ii) a substrate after immersion in a vacuum of 10^{-5} torr (1.3 mPa) at room temperature for 6 h. The vacuum was pumped by oil diffusion.

2.2. Wettability contact angle and surface energy measurements

The wettability contact angle was measured through the sessile drop method [3] on a face contact

0957–4522

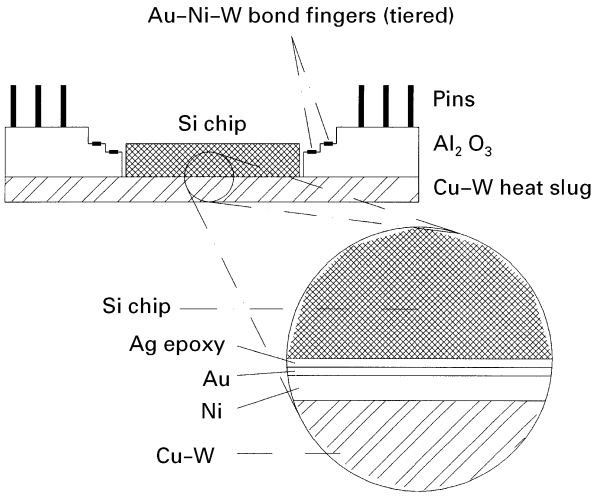

Figure 1 Schematic of a CPGA substrate with a silicon chip mounted on the die attach pad, the central portion of the heat slug. Epoxy bleeding occurs on the Al_2O_3 walls near to the chip.

goniometer (Kyowa Interface Science, model CA-A). The medium used for calculating the surface energy was deionized water (DI water) and methylene iodide. The contact angle measurement was performed on a substrate (from lot A) and on a substrate after vacuum baking (also from lot A). In order to make the measurement, the die pad area of a package was separated from the ceramic substrate by chipping away the sidewalls. A horizontal profile projector at $\times 20$ magnification was used to measure the equilibrium contact angle. By repeating the measurements on several specimens of each type, their consistency was investigated and found to be consistent within a precision of 3°. Computation of the surface energy, γ was based on a method of Wu and Brzozowski [4]. The surface energy of the solid is the sum of the surface dipole component, γ_S^p, and the surface dispersion component, γ_S^d. These are related to the contact angle, θ, through the formula:

$$(1 + \cos\theta)\gamma_L = 4\left(\frac{\gamma_L^d\gamma_S^d}{\gamma_L^d + \gamma_S^d} + \frac{\gamma_L^p\gamma_S^p}{\gamma_L^p + \gamma_S^p}\right) \qquad (1)$$

where γ_L is the surface tension of the liquid used in wetting; as before, it is of the sum of the dispersion component and the polar component. If all the components of γ_L are known for two liquids, then two corresponding measurements of the contact angle will make it possible to solve for γ_S^d, γ_S^p etc., by the solution of a quadratic equation derived from Equation 1.

3. Results

3.1. Auger analysis

Fig. 2 shows typical Auger spectra taken from a raw substrate of lot A. The etching times were 0 and 5 s. The elements detected on the surface are Au, S, C, N and O. After 5 s etching, three of the contaminants, C, N and O – disappeared, but a trace of sulphur on

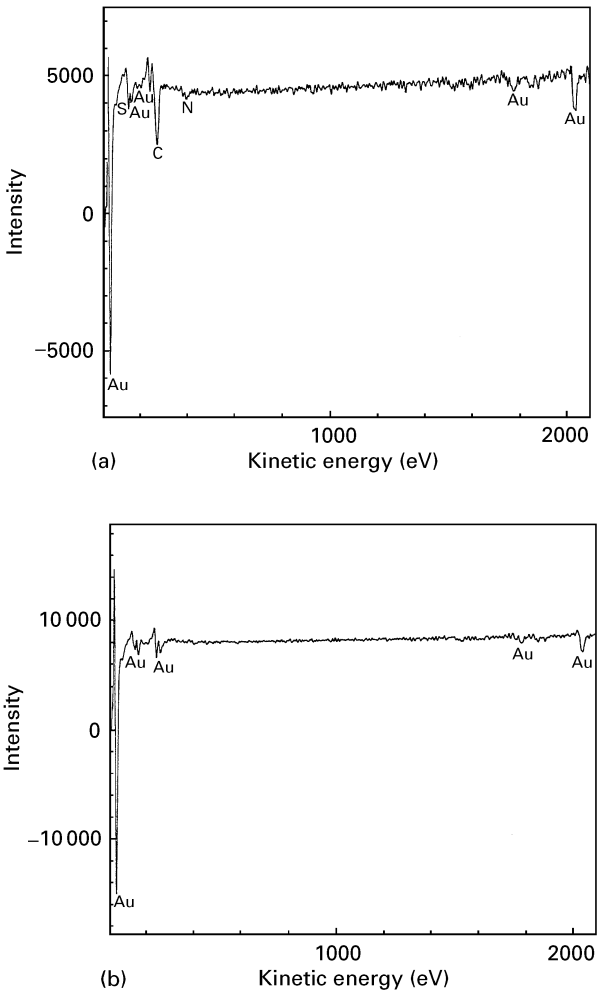

Figure 2 Auger spectra generated from the die attach pad of a raw CPGA substrate from lot A after etching times of (a) 0 s and (b) 5 s.

the subsurface was estimated to be at a mean depth of 1.25 nm below the original top surface.

Fig. 3 shows the Auger spectra taken on the substrate from lot A after vacuum baking. Etching times were 0, 10 and 20 s. Compared with the raw substrates, notice that the carbon contamination is much greater. Carbon continues to be observed even after 20 s of etching (equivalent to an etching depth of ~ 5 nm), showing that the thickness of the carbon film is much increased by the baking procedure.

Auger spectra were taken on the substrate from lot A after baking only in air. Etching times of 0 and 5 s, (Fig. 4) and 10 s (similar to Fig. 4b) were applied. Notice that the carbon contamination has disappeared after 5 s of etching. The carbon contamination level is comparable with that on the raw substrate. However, traces of nickel and oxygen are detected on the top surface. These apparently result, respectively, from diffusion of subsurface nickel during the bake and from its oxidation by air. Results of quantitative analysis on the samples from lot A are listed in Table I.

Fig. 5 shows Auger spectra from the substrate surface before and after evacuating at room temperature. There is no significant difference in carbon contamination on the surface. Table II shows the quantitative analysis.

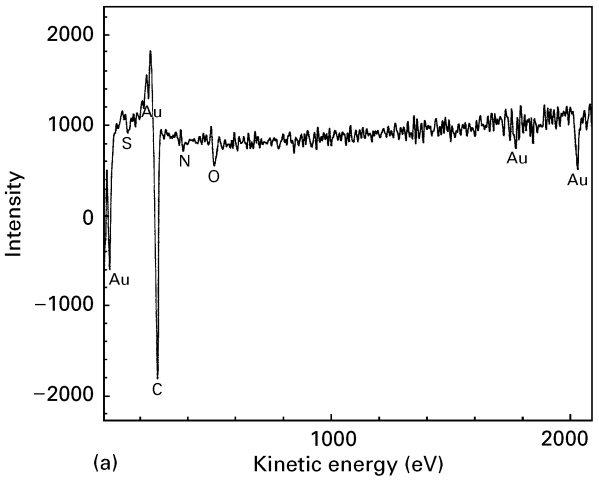

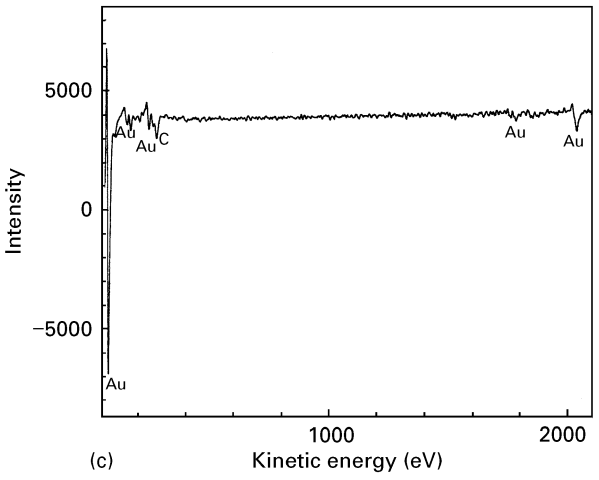

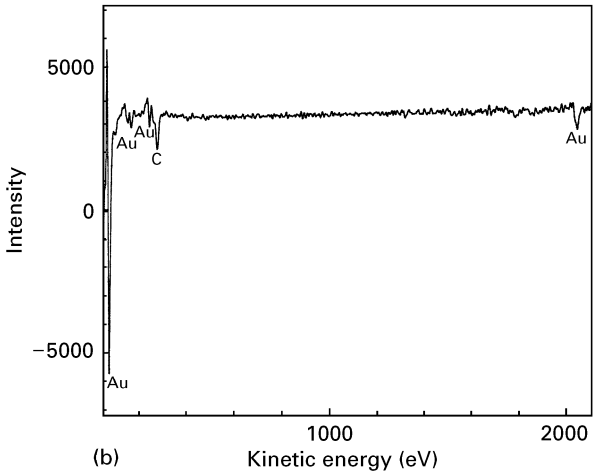

Figure 3 Auger spectra generated from the die attach pad of a CPGA substrate from lot A after vacuum baking and after etching times of (a) 0 s (b) 10 s and (c) 20 s.

3.2. Contact angle measurement and surface energy computation

The measurement and computational results from a raw substrate in lot A, i.e. before vacuum baking and after vacuum baking are listed in Table III. These measurements minimized possible variations due to surface morphology by comparing measurements from specimens of the same lot; and any variations could be ignored for the further reason that gold-plated surfaces are sufficiently dense. A significant increase in the carbon signal is observed after baking. Meanwhile the solid surface energy decreases, especially the polar component. The observed decrease in surface energy is consistent with known surface energies from typical hydrocarbons, such as paraffin tetradecane (25.6 mJ m^{-2}), so the surface energy of the contaminated surface (33.6 mJ m^{-2}) lies between that value and the surface energy of the as-received surface, (41.1 mJ m^{-2}). Thus the effective polarity of the substrate is reduced by the separation from the liquid drop provided by the insulating hydrocarbon film. This is also consistent with the knowledge that hydrocarbons prevent the spreading of water on gold [5], even at a coverage of one monolayer. The surface energy, as measured, is much less than the known surface energy of gold, 1510 mJ m^{-2} [6]. The surface energy of gold is comparatively very high, indicating

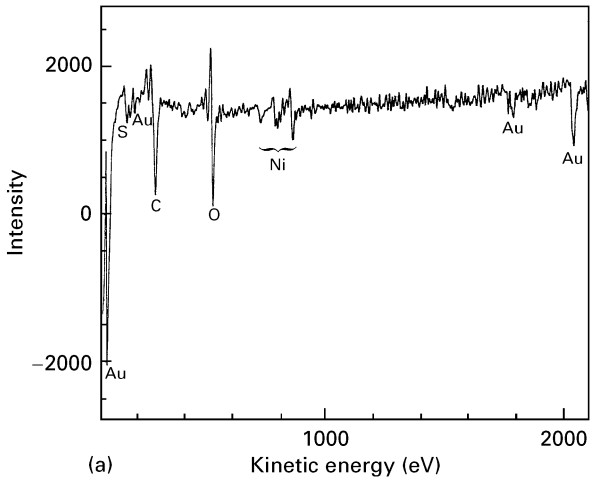

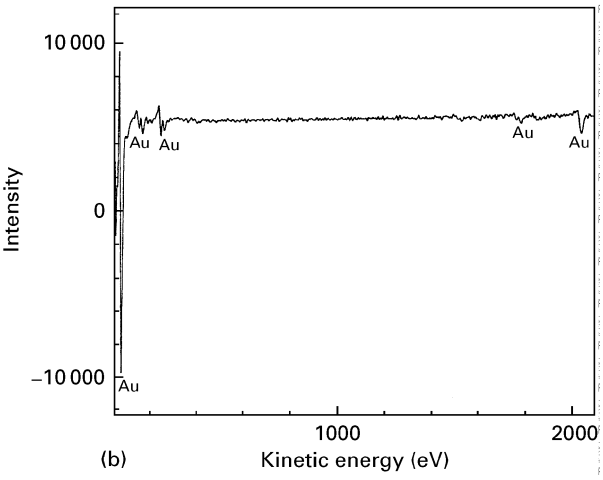

Figure 4 Auger spectra generated from the die attach pad of a CPGA substrate from lot A after baking only in air and after etching times of (a) 0 s and (b) 5 s. After etching for 10 s the spectrum was similar to (b).

the importance of the surface film on wettability. The polar interaction of the gold surface is clearly reduced by atmospheric contamination (water vapour and organics). And on baking, the non-polar oil vapour further reduces the polar interaction.

TABLE I Elemental analysis of CPGA surface calculated from Auger spectra: sample A

Etching time (s)	Etched thickness (nm)	Chemical concentration (at %)					
		Au	O	C	S	N	Ni
Raw							
0	–	58	–	34	4	4	–
5	1.25	100	–	–	–	–	–
Vacuum baked							
0	–	33	4	57	1	5	–
10	2.5	66	–	34	–	–	–
20	5.0	76	–	24	–	–	–
Baked in air							
0	–	45	20	27	2	2	4
5	1.25	100	–	–	–	–	–
10	2.5	100	–	–	–	–	–

TABLE II Elemental analysis of CPGA surface calculated from Auger spectra: sample B

Etching time (s)	Etched thickness (nm)	Chemical concentration (at %)				
		Au	O	C	N	S
Raw substrate						
0	–	45	–	51	3	1
5	1.25	100	–	–	–	–
10	2.5	100	–	–	–	–
Ambient evacuated						
0	–	45	–	51	2	2
5	1.25	100	–	–	–	–
10	2.5	100	–	–	–	–

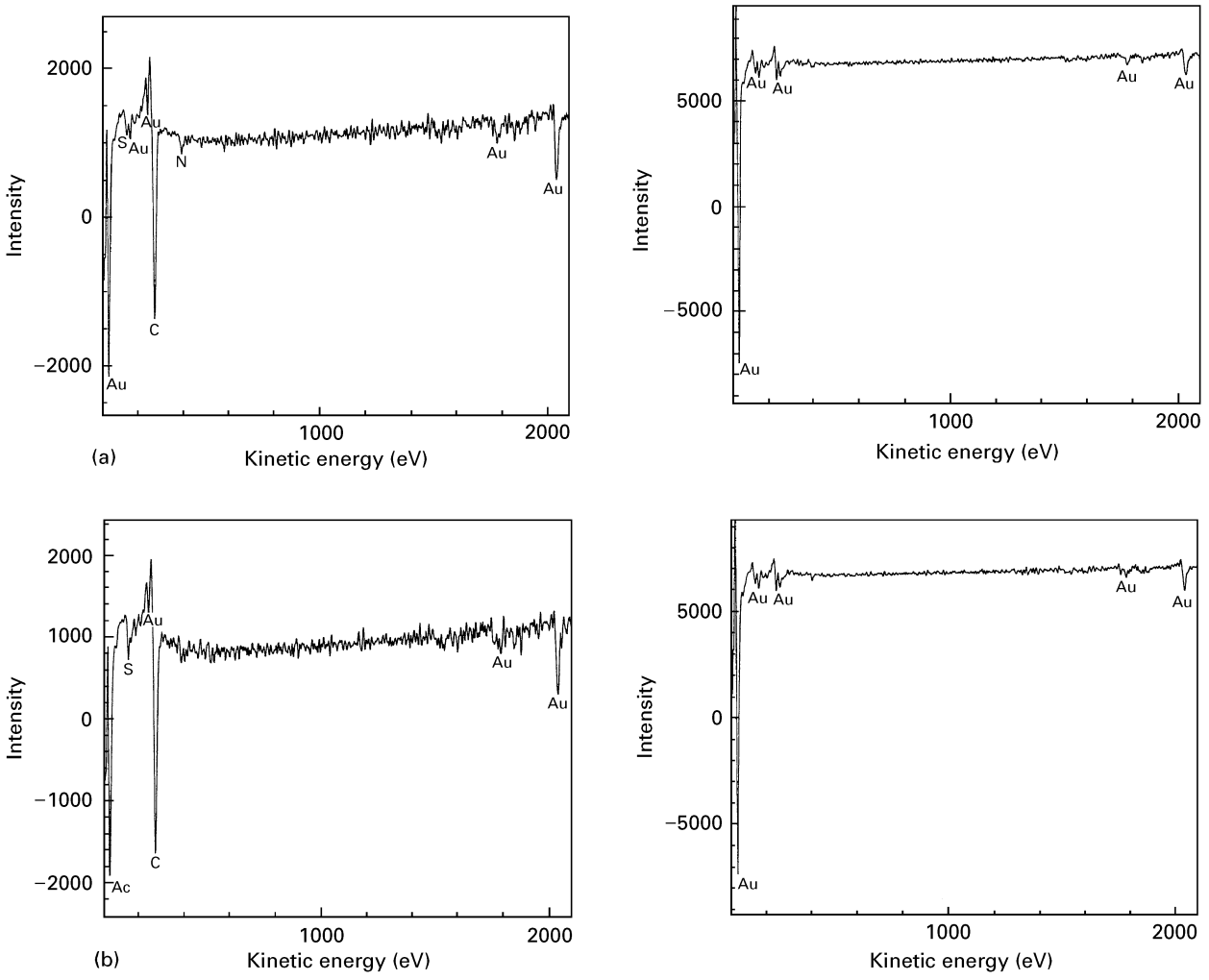

Figure 5 Auger spectra generated from the die attach pad of a CPGA substrate from lot B (a) before and (b) after evacuation in a vacuum of 10^{-5} torr (1.3 mPa) for 6 h using etching times of (left) 0 s and (right) 5 s. After etching for 10 s the results were similar to (right).

4. Discussion

The Auger results show that the carbon contamination is greatly enhanced after standard procedures of vacuum baking. Oil from the rotary vacuum pump typically backstreams to the oven and the pore contaminants typically diffuse. The samples are placed in the hot oven then pumped down. Due to thermal gradients, hydrocarbon vapour phase may then preferentially condense onto cold substrate surfaces. This likelihood is consistent with the Auger analysis data on substrates which have been vacuum baked. In confirmation, surfaces which are only exposed to high vacuum at room temperature, but without baking (i.e. without thermal gradients) show insignificant increase in contamination deposition.

However, it is not necessarily advantageous to eliminate the contamination. Hydrocarbon films, deposited onto substrates during vacuum baking, have

TABLE III Equilibrium contact angles and surface energies computed from contact angles with water and methylene iodide[a]

CPGA substrate	Contact angle		Surface energy ($mJ\,m^{-2}$)			
	Water	Methylene iodide	γ_S^d	γ_S^p	γ	Polarity
Raw	76.3	44.8	28.6	12.5	41.1	0.30
Vacuum baked	92.4	54.1	27.9	5.7	33.6	0.17

[a] The surface energy, γ, is the sum of the dispersion component γ_S^d and the polar component γ_S^p. The surface polarity is equal to the ratio γ_S^p/γ.

reduced surface energies (Table III) compared with clean gold surfaces. Surface energy and contact angle are related as in the Young–Dupré equation

$$\gamma_S = \gamma_L \cos\theta + \gamma_{LS} \quad (2)$$

where γ_{LS} is the interfacial tension [7, 8]. When the surface energy is reduced, $\cos\theta$ is correspondingly reduced, generating high contact angles. A high contact angle implies a less wettable surface and therefore depresses spreading phenomena when an adhesive material is applied to the solid surface. Consequently, the resin bleeding, due to epoxy applied for die attachment in electronic packaging substrates, will be inhibited by the coatings. Moreover, since the electroplated gold surfaces have natural porosity, adhesive properties are not seriously degraded by the coating.

This adhesion was tested by experiments on die shear strength. Adhesive strengths greater than $20\,kg\,cm^{-2}$ were measured, consistent with military specifications [9]. And although low wettability is generally accompanied by reduced adhesion, the effects of capillary action, chemical bonding, etc., in these substrates ensure that they retain sufficiently strong adhesion, even when altered by the contamination as measured.

Similar tests were performed on wirebond pull strength. In spite of the surface modification due to the processing, pull strengths greater than 6 g for 1.2 mil (30 μm) diameter gold wires were measured. Thus the contaminated films are sufficiently thin that they have insignificant effect on wirebond strength.

Oil backstreaming is not a controlled process. This explains why the sensitive effects of the contamination result in sporadic yield-losses. However, the process can be controlled by various methods: the composition of residual vacuum gases could be monitored and controlled; the deposition rate could be controlled through temperature-controlled gradients; thermal and vacuum cycling rates could be related to coating levels; or a coating could be added in a controlled way during cleaning and before assembly, etc. The coating can be monitored by wettability measurement and controlled to produce a surface with optimum contact angle and with adequate adhesion.

The surface modification clearly depends on the chosen vacuum system. In our experiments two different systems (rotary-pumped with oil trap as in Table I versus diffusion-pumped with liquid nitrogen trap as in Table II) yielded essentially consistent results. Carbon contamination of the specimens was negligible at ambient temperature in the diffusion-pumped vacuum (compare with the raw and evacuated specimens in Table II); but when specimens were subsequently vacuum baked at 235 °C, increased carbon was analysed on the surface, similar to that shown in Table I but with reduced thickness.

This study illustrates "appropriate cleanliness" which should be used in processing of electronic packages. Very clean ceramic surfaces have high surface energies that are susceptible to epoxy bleeding. Moderate cleaning is compatible with the surface coating needed to reduce the surface energy.

5. Conclusion

Surface analysis and wettability measurements show that hydrocarbons are coated onto packaging substrates during conventional vacuum bakeout. In consequence, the surface energies are typically reduced and standard theory implies that such a reduction in surface energy will help to inhibit epoxy-bleeding. This benefit was confirmed in wettability contact angle measurements. The lack of control during vacuum bakeout explains sporadic yield-loss due to epoxy bleeding, since contamination is a sensitive processing parameter. The analysis indicates how the coatings might be controlled to eliminate the yield-loss due to epoxy bleeding and to optimize, with appropriate cleanliness, the process for an even, reproducible and secure bond.

Acknowledgements

We are grateful to C. Y. S. Tan and to N. H. Lee for facilitating the project. Part of the work was performed under NUS grant RP940637.

References

1. J. E. IRELAND, *Int. J. Hybrid Microelec.* **5** (1982) 1.
2. N. X. TAN, A. J. Y. LEE, A. J. BOURDILLON and C. Y. S. TAN, *Semicond. Sci. Technol.* **17** (1996) 437.
3. C. A. MILLER and P. NEOGI, "Interfacial Phenomena: Equilibrium and Dynamic Effects" (Marcel Dekker, New York, 1980) pp. 54–83.
4. S. WU and K. J. BRZOZOWKSI, *J. of Colloid Interface Sci.* **37** (1971) 686.
5. V. A. PARSEGIAN, G. H. WEISS and M. E. SCHRADER, *ibid.* **61** (1977) 356.
6. W. R. TYSON and W. A. MILLER, *Surf. Sci.* **62** (1977) 267.
7. A. W. ADAMSON, "Physical Chemistry of Surfaces", 2nd Edn (Wiley, New York, 1967).
8. J. J. BIKERMAN, "Physical Surfaces" (Academic Press, London, 1970).
9. Test Methods and Procedures for Microelectronics, MIL-STD-883D, method 2019.5, USA (1993).

Received 7 May
and accepted 26 July 1996